




Article

Analysis of Grid-Interactive PV-Fed BLDC Pump Using Optimized MPPT in DC–DC Converters

Jeba Singh Oliver ¹, Prince Winston David ^{2,*} , Praveen Kumar Balachandran ³  and Lucian Mihet-Popa ^{4,*} 

¹ Department of EEE, Arunachala College of Engineering for Women, Kanyakumari 629203, India; o.jebasingh@rediffmail.com

² Department of EEE, Kamaraj College of Engineering and Technology, Virudhunagar 625701, India

³ Department of EEE, Vardhaman College of Engineering, Hyderabad 501218, India; praveenbala038@gmail.com

⁴ Faculty of Information Technology, Engineering and Economics, Oestfold University College, 1757 Halden, Norway

* Correspondence: dpwtce@gmail.com (P.W.D.); lucian.mihet@hiof.no (L.M.-P.)

Abstract: In solar photovoltaic (PV) system-based Brushless DC (BLDC) motors for water pumping application, the role of DC/DC converters is very important. In order to extract the maximum power from the PV array, an efficient DC/DC converter is essential at the intermediate stage. In this work, different DC/DC converter topologies suitable for BLDC motors are proposed. The converters are supported by an optimized maximum power point tracking system to provide a reliable operation. Recent optimization algorithms such as fuzzy logic, perturb and observe, grey wolf, and whale optimization are implemented with the PI controller in maximum power point tracking to maximize the conversion efficiency. The obtained results using SEPIC, LUO, and interleaved LUO converters provide a comparative study in the case of converter output, motor parameters, and grid output. The performance analysis on three different converters and multiple optimization methods are carried out. By analyzing the performance of different converter topologies, the interleaved LUO converter outperforms the other two converters with the results of a voltage gain ratio of 1:22, conversion efficiency of 98.3%, and grid current THD of 2.9%. Moreover, regarding the power quality aspect, the total harmonic distortion of the grid current is maintained below the IEEE-519 standard. In addition, the developed system has an advantage of operating both in stand-alone and grid-connected operation modes.

Keywords: solar photovoltaics; brushless DC motor; maximum power point tracking; DC–DC converter



Citation: Oliver, J.S.; David, P.W.; Balachandran, P.K.; Mihet-Popa, L. Analysis of Grid-Interactive PV-Fed BLDC Pump Using Optimized MPPT in DC–DC Converters. *Sustainability* **2022**, *14*, 7205. <https://doi.org/10.3390/su14127205>

Received: 10 May 2022

Accepted: 7 June 2022

Published: 13 June 2022

Publisher's Note: MDPI stays neutral with regard to jurisdictional claims in published maps and institutional affiliations.



Copyright: © 2022 by the authors. Licensee MDPI, Basel, Switzerland. This article is an open access article distributed under the terms and conditions of the Creative Commons Attribution (CC BY) license (<https://creativecommons.org/licenses/by/4.0/>).

1. Introduction

Due to the increased population and global warming, the conventional energy sources are decreasing rapidly, and people are shifting toward the usage of renewable energy sources [1]. The PV modules are widely used in many applications, which can be used as a grid-interactive system or standalone system. The PV system converts the energy received from the sun into dc power. The output of the PV array is affected due to different atmospheric conditions such as temperature, intensity, and shading of clouds. The output of the PV is tested under standard test conditions. To obtain the desired voltage level, the PV cells are connected in series, and in order to increase the current level, the PV cells are connected in parallel. The operating voltage of the PV array is maintained at a rated value using MPPT. The model of a PV cell consists of a battery, shunt resistance, diode, and a series resistance. The load is connected across the cell and the operating point is at the intersection point of the load and volt-ampere characteristics of the cell.

Normally, water pumps are used to raise the water to a higher altitude. In our work, a Brushless DC motor (BLDC) is utilized for a DC water pumping application [2]. It has several advantages such as simple construction, less maintenance, operation in synchronous

speed, and superior electrical and mechanical characteristics. Under both no load and loaded conditions, the BLDC motor produces high torque and is able to run faster. At the same time, the speed of the motor varies due to the variation in the generated PV power [3]. As the conversion efficiency of the PV panel is low, a maximum amount of power is drawn through efficient Maximum Power Point Tracking (MPPT) algorithms. In addition, a DC-to-DC power conversion is essential to change the DC power into another available DC voltage level. Different existing DC-to-DC converter topologies are Buck, Boost, Buck–Boost, CUK converter, etc. However, the existing converters produce switching losses; hence, it requires a converter with high output gain and soft switching performance [4]. Therefore, the selection of a suitable DC/DC converter is a major task in PV-fed BLDC motor systems.

Considering the above issues, in this proposed scheme, an analysis is made to study the performance of different converter topologies suitable for a PV-fed three-phase BLDC motor. In the proposed work, the SEPIC, LUO, and interleaved LUO converters that are suitable for the BLDC motor in water pumping application are considered. In addition, a control scheme is needed to control the output of the converter operated with MPPT systems. Therefore, a control scheme using the PI controller is applied for achieving a steady-state operation in MPPT. The drawback such as the peak overshoot problem leads to the discovery of optimization-based methods. The conventional PI controller increases the nonlinearity and parametric variation in load. Accordingly, the recent optimization tools such as fuzzy logic, Perturb and Observe (P&O), Grey Wolf (GW), and Whale Optimization (WO) techniques along with the PI controller are implemented in order to achieve the desired output without any delay. The aim of this study is to improve the efficiency in the BLDC motor with less energy consumption, reducing the oscillatory current in the motor as well as eliminating commutation problems. Moreover, the power quality is maintained in the grid under standalone and grid-interactive operation of the PV-fed BLDC motor [5]. The remaining part of this paper is summarized as follows: Section 2 demonstrates the review of the literature; Section 3 explains in detail the stages of the proposed system; and Section 4 demonstrates the results with the comparative analysis. Finally, Section 5 presents a brief conclusion about the work.

Objectives of the proposed work are given below:

- To regulate the speed of the BLDC motor using a closed-loop PI controller and Hall sensor.
- To boost the PV array output with high gain, low ripples, and minimum power loss.
- To extract maximum power under varying irradiance conditions using the MPPT system with the optimized PI controller.
- To create a grid-interactive system to supply power during the night and receive excess solar power at daytime.
- To minimize the THD of the grid current below 5%.

2. Review of Literature

Though much literature is available in water pumping systems using BLDC motors, MPPT, DC/DC topologies, and grid-interactive systems, a few studies from the literature relevant to the proposed work are discussed in this section. According to Shadab et al. [6], a modified vector control is applied on a permanent-magnet synchronous motor operated with a standalone PV array system. In this system, the utilization of a DC/DC converter at the intermediate stage is avoided, even though this method is time-consuming without a FET. Furthermore, in [7], a two-stage energy conversion system is adopted in a solar-fed reluctance synchronous motor for a water pumping system. A boost converter optimized using the incremental conductance method is coupled with the PV to increase the output. Though it improves the reliability and power factor, the maximum power decreases when the solar irradiation changes. Moreover, Saurabh et al. [8] highlights an ANN-based reliable model in the PV and grid-integrated induction motor drive. Here, a reference adaptive system will estimate the flux and regulate the power. Elimination of harmonic contents

and the offset voltage adds an advantage to the system. In addition, Riccardo et al. [9] introduces a permanent-magnet synchronous motor-driven water pump controlled by a field-oriented control. The controller will modify the reference speed of the motor to achieve a superior MPPT operation. This scheme is easy to install that reduces the number of stages, cost, and complexity. However, if the feed-forward accelerator is added at the speed control, it gives a distinctive trait.

According to Zhang et al. [10], a buck converter is used for regulation of the speed drive and reduction of torque ripples by Pulse-Width Modulation (PWM) chopping techniques. Later, in [11], boost converter configurations contribute more to BLDC drives. Due to the high-frequency PWM signal, switching losses will occur in Voltage Source Inverters (VSIs). Hence, CUK converters are used to reduce the switching losses and control the speed of the motor drive as a function of the VSI [12]. In addition, Kumar and Singh [13] implement a buck–boost converter in a BLDC water pumping system with soft starting features. Still, a few problems exist such as discontinuous output current, ripples, and switching loss in the VSI. Furthermore, in [10], a zeta converter is discussed where the switching sequence of the VSI is controlled by the PWM pulse. Again, the switching loss problem occurs in the zeta converter. Moreover, in [11], an MPPT-based CUK converter is designed in combination with a PV-fed BLDC motor. Therefore, the ripples are eliminated, and variable speed control is also achieved. Recently, a few optimization techniques such as fuzzy and Artificial Bee Colony algorithms are added in [12] to improve the performance of the MPPT in similar applications with the zeta converter.

Additionally, a fuzzy-based PID controller is used to control the speed of the BLDC motor to control the speed by tracking the reference speed of the rotor [13]. Similar MPPT based pumping systems were discussed in [14,15]. In addition, a PV-fed BLDC motor for a water pumping system without a battery is designed and implemented with a sensorless speed controller with a sliding mode controller (SMC), as highlighted in [16]. The proposed Hybrid Whale Optimization technique works effectively to extract the maximum power from the PV during both partial shading and normal conditions. The obtained results are analyzed with Genetic Algorithm (GA), Particle Swarm Optimization (PSO), and Grey Wolf Optimization (GWO) methods for MPPT; therefore, the overall cost of the system reduces. According to Ovaiz et al. [17], a new technique is developed using the super lift LUO converter to increase the voltage step by step in geometric progression. Therefore, the transfer gain is enhanced, which is suitable for PV applications. In addition, the Cuckoo algorithm is implemented in the MPPT along with the converter.

3. System Design

The block diagram of the proposed system is presented in Figure 1. It comprises components such as a PV array, DC/DC converter, PWM generator, three-phase VSI, single-phase VSI, BLDC motor, PI controller, sensors, and a driver circuit.

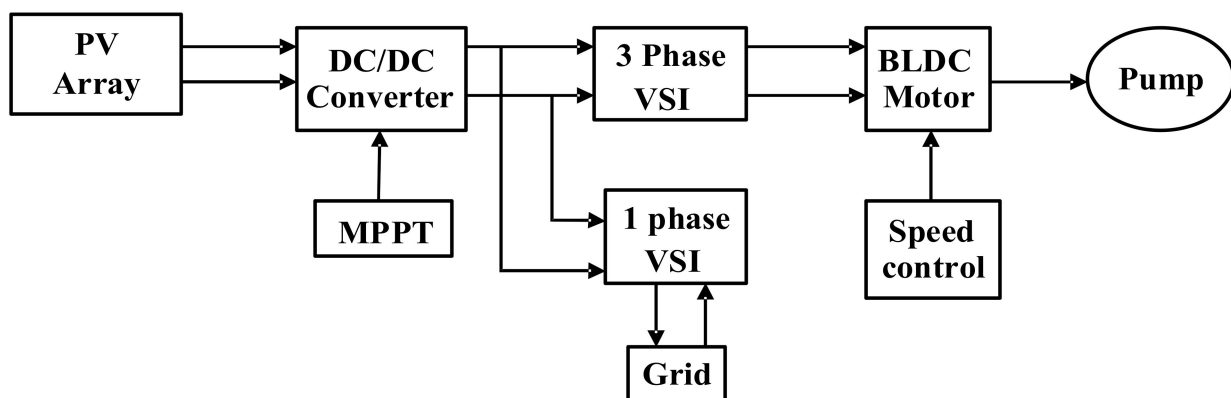


Figure 1. Proposed block diagram of grid-interactive PV-fed BLDC pump.

3.1. BLDC Motor

The BLDC motor is a similar version of the synchronous motor with a smaller size that exhibits linear characteristics between current and torque. According to the construction of the BLDC motor, the stator consists of a 3-phase steel-laminated core with 3 sets of stator windings. In addition, the rotor contains a permanent magnet with a fixed number of poles. The BLDC motor can be operated in sensor mode or sensorless mode. In the case of the sensorless BLDC motor, it has many advantages such as no sensing part, reduced size, and less cost. However, it requires a control algorithm and an electronic control circuit, which is quite complex. Moreover, instead of using brushes in a BLDC motor, the power switches are used as electronic commutation. Accordingly, the two chosen winding motors energize in 6 positions, or 6 steps, and the rotor position will coincide in any of the six stages of the inverter.

3.2. Speed Control of BLDC Motor

Speed control of the BLDC motor is essential for operating a centrifugal water pumping system [18]. This speed control can be performed either through sensors or a sensorless method. Although the sensorless method has a few advantages such as reduced size and low cost, it requires complex electronic circuits and algorithms. Therefore, in this method, a Hall sensor is used to measure the actual speed of the BLDC motor. The actual speed is compared with the reference speed and the error value is given to the PI controller. The closed-loop arrangement becomes activated once the steady state is reached. In addition, two gain values are initialized depending on the two variables such as error of current and the new speed. Thus, tuning the proportional and integral gain values in such a way by fixing the half value for proportional gain and adjusting the integral gain, the PWM pulses are generated. The driver circuit will feed the generated PWM pulses to the three-phase voltage source inverter. Therefore, the speed regulation is achieved and the control diagram for speed control is shown in Figure 2.

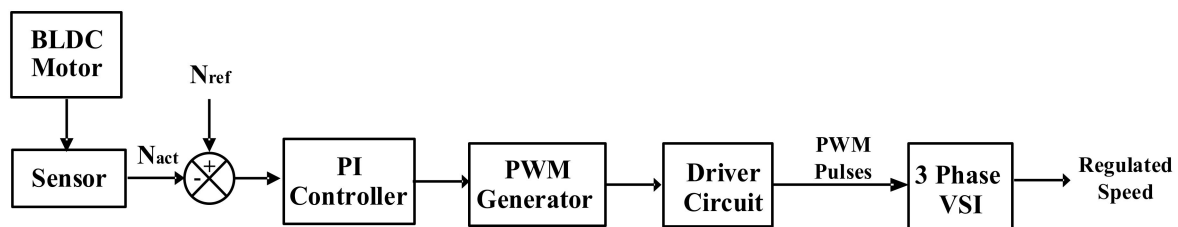


Figure 2. Speed control scheme for BLDC motor.

3.3. DC/DC Converter

The output of the PV array is coupled with the BLDC motor through a DC/DC converter. The DC/DC converter is chosen with a high gain so that the number of solar panels can be reduced. The output of the DC/DC converter is fed to the voltage source inverter and is then given to the BLDC pump. In this work, three different converter topologies are selected and tested to analyze the performance of the proposed system.

3.3.1. SEPIC Converter

The Single-Ended Primary Inductor Converter (SEPIC) is characterized with an output voltage greater or equal to the input voltage. The voltage gain ratio of a SEPIC converter is 1:8 and it boosts the input voltage by 8 times. The input and output of the SEPIC converter have the same polarity. The control of the SEPIC converter mainly depends on the duty cycle of the switch. The operation of the SEPIC converter is analyzed in two modes: Mode

1, when switch S is ON, and Mode 2, when switch S is OFF. The topology of the SEPIC converter is shown in Figure 3.

$$\text{The duty cycle, } D = \frac{V_o + V_D}{V_o + V_{PV} + V_D} \quad (1)$$

where V_o is the output voltage, V_D is the voltage drop, and V_{PV} is the supply voltage.

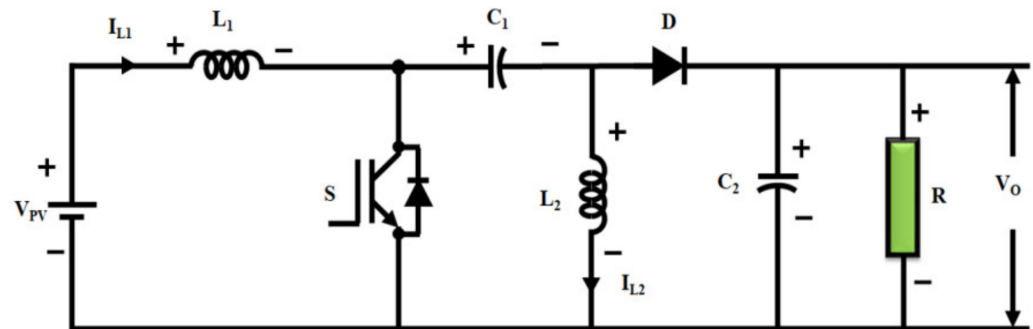


Figure 3. SEPIC converter topology.

3.3.2. LUO Converter

The LUO converter is an advanced version of the DC/DC converter with a gain ratio of 1:12 and the voltage is boosted 12 times. As the gain ratio is greater than that of the SEPIC converter, the number of solar panels can be further reduced. The LUO converter provides a positive output for higher voltage levels. The advantages such as simple topology, high efficiency, and high power density make it more suitable for PV applications. The topology of the LUO converter is depicted in Figure 4.

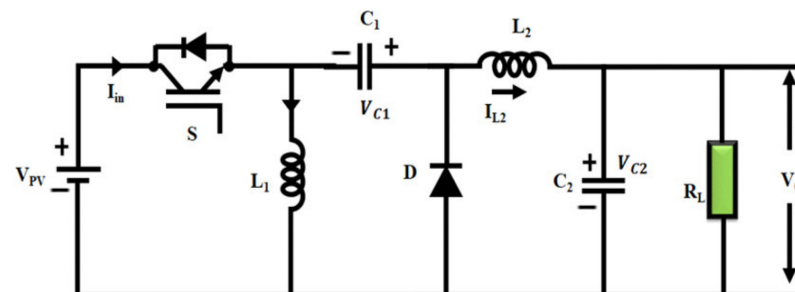


Figure 4. LUO converter topology.

The maximum and minimum values of duty cycles are evaluated by,

$$D_{\max} = \frac{V_o + V_D}{V_o + V_{PV\min} + V_D} \quad (2)$$

$$D_{\min} = \frac{V_o + V_D}{V_o + V_{PV\max} + V_D} \quad (3)$$

3.3.3. Interleaved LUO Converter

Here, the interleaving refers to the two converters connected in parallel at the input side and connected in series at the output side. In such a way, two LUO converters are connected in an interleaved way such that the switches operate 180 degrees out of phase. This converter will boost the output of the PV system with high efficiency, low ripples, and minimum power loss. The output of the converter is interconnected with the BLDC pumping system through a three-phase VSI. The topology of the interleaved LUO converter is shown in Figure 5.

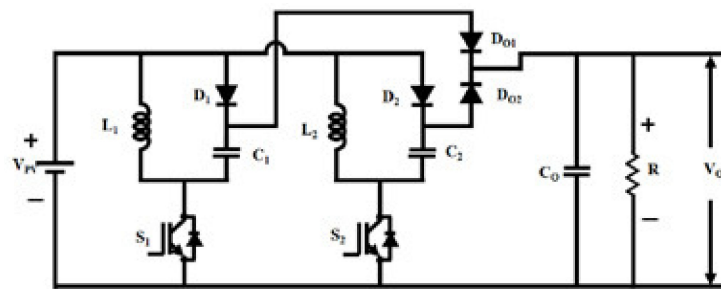


Figure 5. Interleaved LUO converter topology.

3.4. MPPT in PV-Fed BLDC

Due to the change in environmental factors and weather conditions, maximum power point tracking algorithms are extensively used for the extraction of maximum available power in the present scenario. It is essential that the PV arrays are operated at the maximum power point level because of the expensive solar cells. A maximum power point tracker is used to track the maximum power point axis of the PV array. The load line must correlate with the maximum power point axis of the PV array for overall efficient working of the system. This load line point may change with respect to temperature, solar radiation, and loading conditions. Therefore, the maximum power point must be tracked continuously to respond to the fast changes. Any one of the controlling methods such as open-loop control or closed-loop control can be adopted for such types of problems. The closed-loop control operation of MPPT with PI is implemented accordingly, as shown in Figure 6.

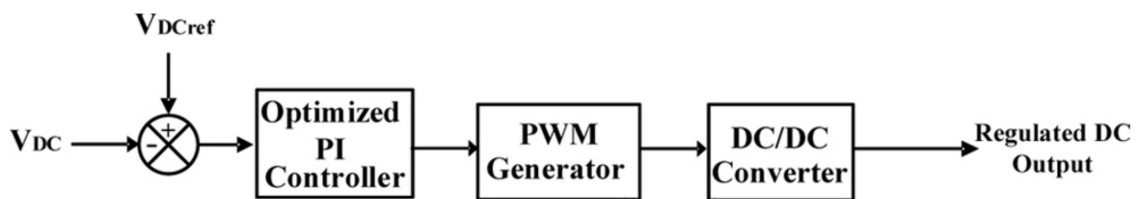


Figure 6. MPPT control scheme in DC/DC converter.

To perform the closed-loop operation in MPPT, the voltage across the DC capacitor present in the DC/DC converter is monitored and is then compared with the reference voltage across the DC link capacitor. The error voltage signal is given to the PI controller where the gain parameters are tuned using the different optimization algorithms. The optimally tuned controller produces a reference signal. This reference signal is analog with the carrier signal to generate the pulses by the PWM generator. Finally, switching of the converter takes place and the regulated DC output is delivered to the BLDC motor.

3.4.1. PI Controller

The PV array is coupled with the BLDC motor through a DC–DC converter and the control of the converter is carried out with a PI controller [19]. The control of the converter is carried out with the help of a PI controller, but there exist problems with peak overshoot and settling time. To find the optimal values of the K_p and K_i gains, manual tuning is made by fixing the integral gain to its maximum value and the term of derivation to zero and by increasing the proportional gain until the loop oscillates at a constant amplitude. By setting the proportional gain to half value and by adjusting the integral gain, the offset within an acceptable period is corrected.

3.4.2. P&O Optimization

In MPPT, the P&O method can be employed in two ways: (i) by modifying the output of the PV module according to the reference using the PI controller; and (ii) by adjusting the duty ratio of the DC/DC converter to extract the maximum output power of the PV

module. The second method is advantageous so that it can respond to slow changes in irradiance and temperature. Still, the drawbacks such as slow convergence speed and oscillations in the steady-state output may cause deviations in the operating point from the maximum power point [20].

3.4.3. Fuzzy Logic

In order to maximize the power at any climatic condition, as well as to improve the efficiency of the P&O algorithm, an intelligent fuzzy-based MPPT is implemented [21]. The error and change in error are the two inputs given to the fuzzy controller. In the fuzzification stage, the input signals are assigned with fuzzy values. In the inference system, a collection of if then rules under the Mamdani method is applied along with min-max operation. Finally, the inference rules are converted in non-fuzzy (crisp) data, which is necessary for the control process.

3.4.4. Grey Wolf Optimization

The grey wolf optimization was proposed by Mirjalili [22] in 2014. The GW algorithm follows the social behavior of grey wolves while hunting preys. There exist a few categories of wolves in the wolf pack such as alpha, beta, delta, and omega. They are categorized based on their strength and fitness. The wolf with full fitness is known as alpha and the other wolves having a fitness close to alpha are named as beta and delta. The remaining wolf is termed as omega. This pack of wolf structure will perform the hunting by the process of tracking, encircling, and attacking. Likewise, in the GW model, the available solution is grouped into several categories close to the desired output. Then, we move toward the final solution. Finally, the optimum solution is reached by the alpha.

3.4.5. Whale Optimization

This is a meta-heuristic algorithm, which initiates the hunting character of humpback whales. In this method, the hunting process is performed by the popular search assistant that searches the prey and uses the bubble net mechanism of the humpback whales. This hunting mechanism is executed in three steps. In the first step, the prey location is identified and is encircled. If not, according to the WO algorithm, the greatest solution of the candidate at present is aimed at the prey. Therefore, the search assistants will enhance the search and update a new location. Secondly, the bubble net attacking is framed by two mechanisms: the mechanisms of shrinking encircle and spiral updating position. The last phase is the exploration stage, in which the chasing of the prey is performed accidentally. The whales accidentally look at each other's position and enhance their position according to the selected assistant. In case of MPPT control, the PI controller is tuned to produce the reference signal, which is used to control the pulses. By applying the pulses to the converter's switches, the steady-state output is maintained [23].

3.5. Grid Control

In general, for a PV system, the DC/DC converter with a high gain is essential. One such type of converter is the interleaved LDO converter with a voltage gain ratio of 1:22. During the night, solar power is not available, so the BLDC pump is driven by the grid power. Likewise, during daytime, the excess power from the solar panel can be fed to the grid through another single-phase VSI [4]. In this scheme, the grid power and the reference power are compared and the error signal is given to the PI controller shown in Figure 7. The PI control scheme regulates the grid power and is fed to the grid through a single-phase VSI. The PWM generator provides the pulses to control the output of the VSI.

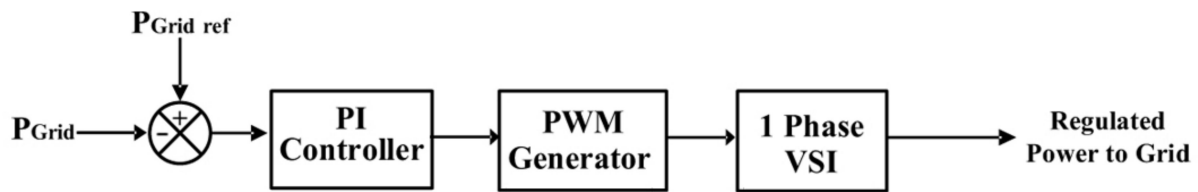


Figure 7. Grid power control scheme.

4. Results and Discussion

The analysis of the proposed grid-interactive PV-fed BLDC pumping system is analyzed under various steady-state and dynamic conditions. The model of the system is developed and tested using the MATLAB-Simulink software package with the specifications given in Table 1.

Table 1. Specifications of the BLDC motor.

Number of poles	4
DC voltage	270 V
Power rating	1.5 KW
Grid voltage	200 V

4.1. Solar Panel Outputs

The measured readings of the maximum irradiation level, output voltage, output current, and output power with respect to different converters such as SEPIC, LUO, and interleaved LUO are presented in Table 2.

Table 2. Output of solar panels connected with different converters.

Output	SEPIC		LUO		Interleaved LUO	
	t < 0.1 s	t > 0.1 s	t < 0.1 s	t > 0.1 s	t < 0.1 s	t > 0.1 s
Irradiation level (W/m ²)	980	1000	980	1000	980	1000
Voltage (V)	110	120	80	100	78	80
Current (A)	12.5	13	14	15	17.25	18.75
Power (W)	1360	1500	1250	1500	1360	1500

4.2. Converter Outputs

The regulated DC output of DC-to-DC converters connected with an optimized PI-controlled MPPT and the PWM generator is shown in Figure 8. The MPPT control scheme is developed based on a PI controller and, further, the gain values are optimized to improve the performance of the MPPT as well as to tune the regulated DC output of the converter. The outputs are obtained using the PI controller alone as well as in combination with the P&O, Fuzzy logic, GWO, and WO algorithms.

By noticing the output waveforms of the converter, the settling time of voltage is reduced through different algorithms and the better performance is reached for the WO algorithm. Figure 8 shows the output voltages of SEPIC, LUO, and interleaved LUO converters with PI-controlled MPPT, PI + P&O, PI + Fuzzy, PI + GWO, and PI + WO algorithms. The voltage-gain ratio of the SEPIC converter is 1:8, whereas a high-gain DC-DC LUO converter operates with a gain of 1:12. Further, the implemented interleaved LUO converter has a voltage-gain ratio of 1:22.

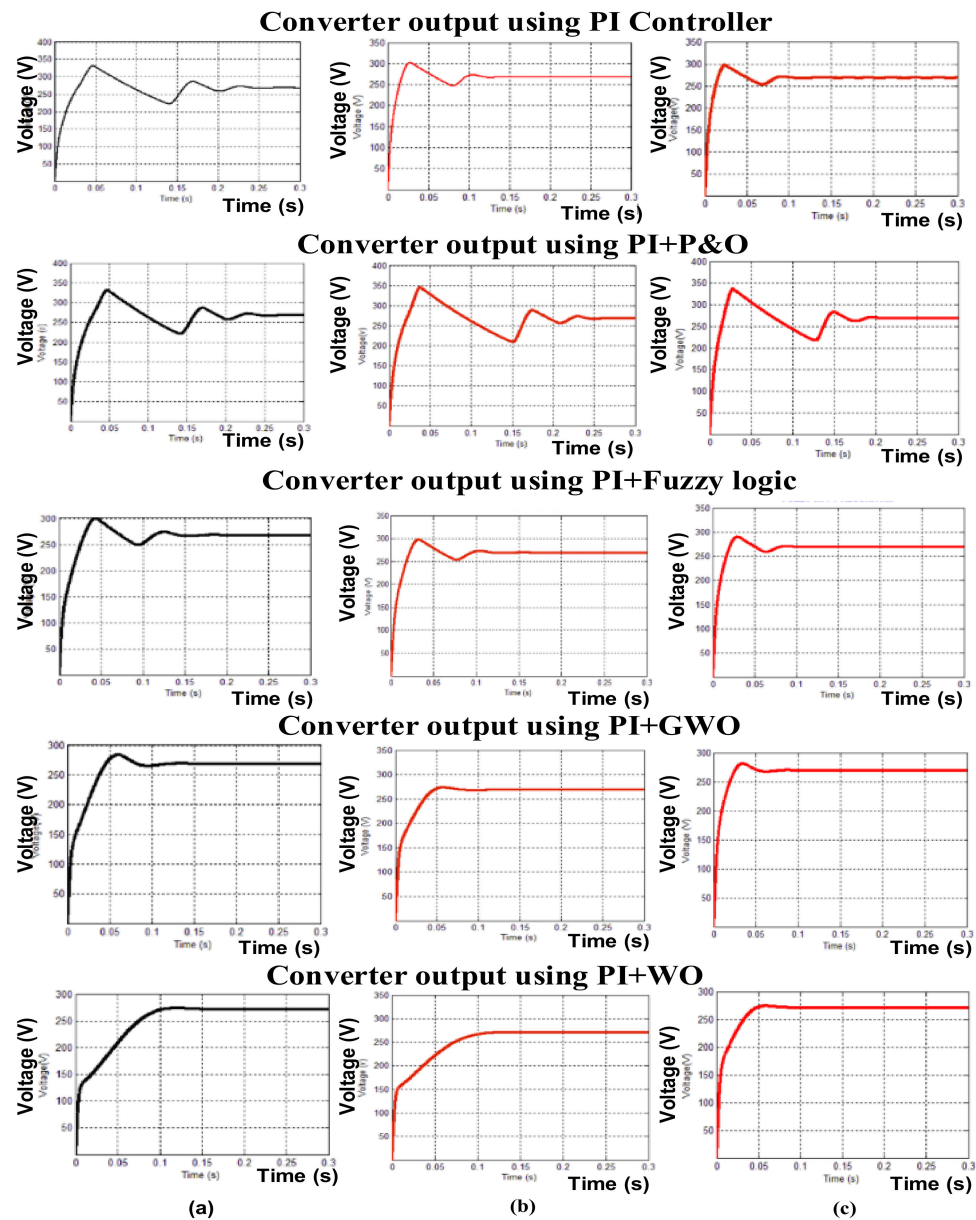


Figure 8. Output of different converters with optimized PI-controlled MPPT: (a) SEPIC, (b) LUO, and (c) interleaved LUO converters.

Moreover, the settling times of each converter output with different MPPT schemes are tabulated in Table 3. Likewise, the conversion efficiency of different converters with various control schemes is presented in Table 4. The settling time reduces gradually with PI and improved regulation is reached by tuning the optimization methods.

Table 3. Settling time of different converter outputs with various MPPT control schemes.

Control Schemes of MPPT	SEPIC(s)	LUO(s)	Interleaved LUO(s)
PI	0.30	0.25	0.20
PI + P&O	0.25	0.20	0.10
PI + Fuzzy	0.20	0.16	0.10
PI + GWO	0.15	0.13	0.09
PI + WO	0.10	0.12	0.08

Table 4. Conversion efficiency of different converters with various MPPT control schemes.

Converters	MPPT Control Schemes	Efficiency (%)
SEPIC	PI + P&O	87
	PI + Fuzzy	89
	PI + GWO	93
	PI + WO	94.6
	PI + P&O	92
LUO	PI + Fuzzy	94
	PI + GWO	95.8
	PI + WO	96.2
	PI + P&O	95.4
INTERLEAVED LUO	PI + Fuzzy	96.7
	PI + GWO	97.5
	PI + WO	98.3

4.3. BLDC Motor Output

In this section, the starting nature of the BLDC motor with different converters and the steady-state operation under different operating conditions are discussed.

The results are obtained during the starting condition from 0 to 0.1 s, the running condition from 0.1 to 0.3 s, and the dynamic loading condition from 0.25 to 0.3 s. The essential motor parameters such as current, back emf, speed, and torque are acquired under each operating condition. The obtained waveforms of the BLDC motor parameters under starting, running, and loading conditions using the SEPIC converter are depicted in Figure 9a–c, respectively. Likewise, the BLDC motor output using the LUO converter is presented in Figure 10a–c, respectively. Similarly, the output of the BLDC motor using the interleaved LUO converter is shown in Figure 11a–c, respectively.

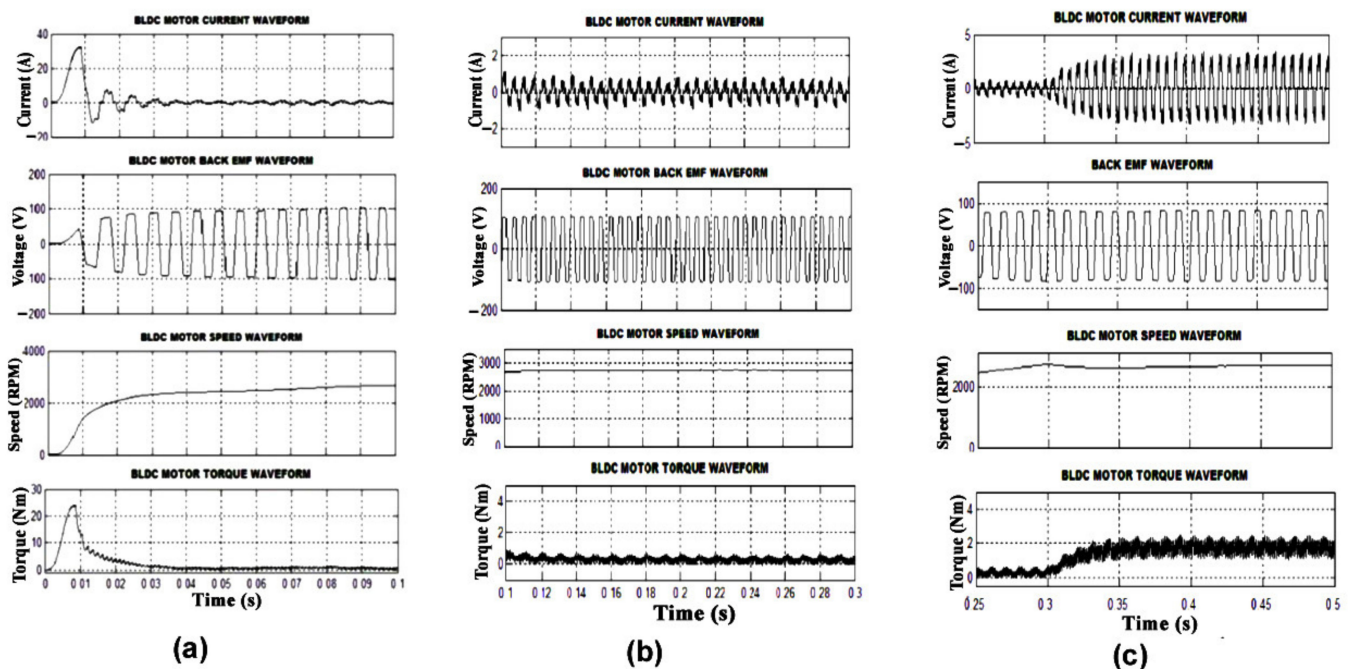


Figure 9. BLDC motor parameters with SEPIC converter under (a) starting, (b) running, and (c) loading conditions.

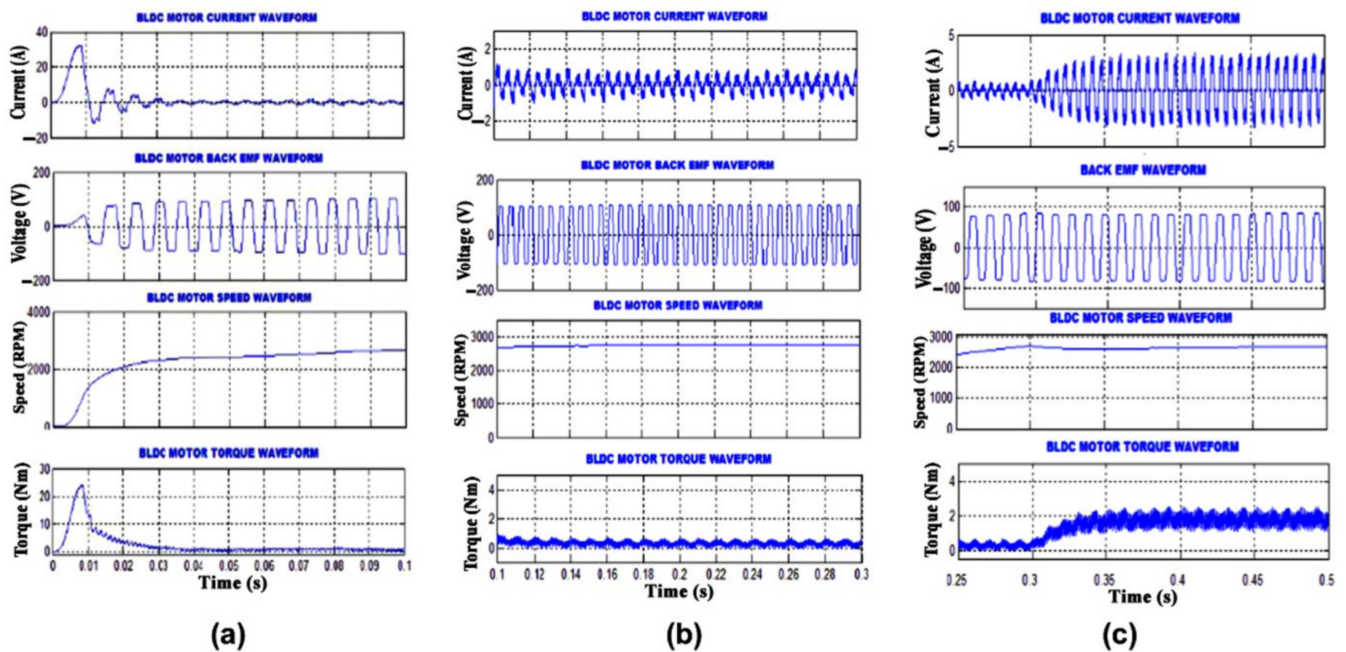


Figure 10. BLDC motor parameters with LUO converter under (a) starting, (b) running, and (c) loading conditions.

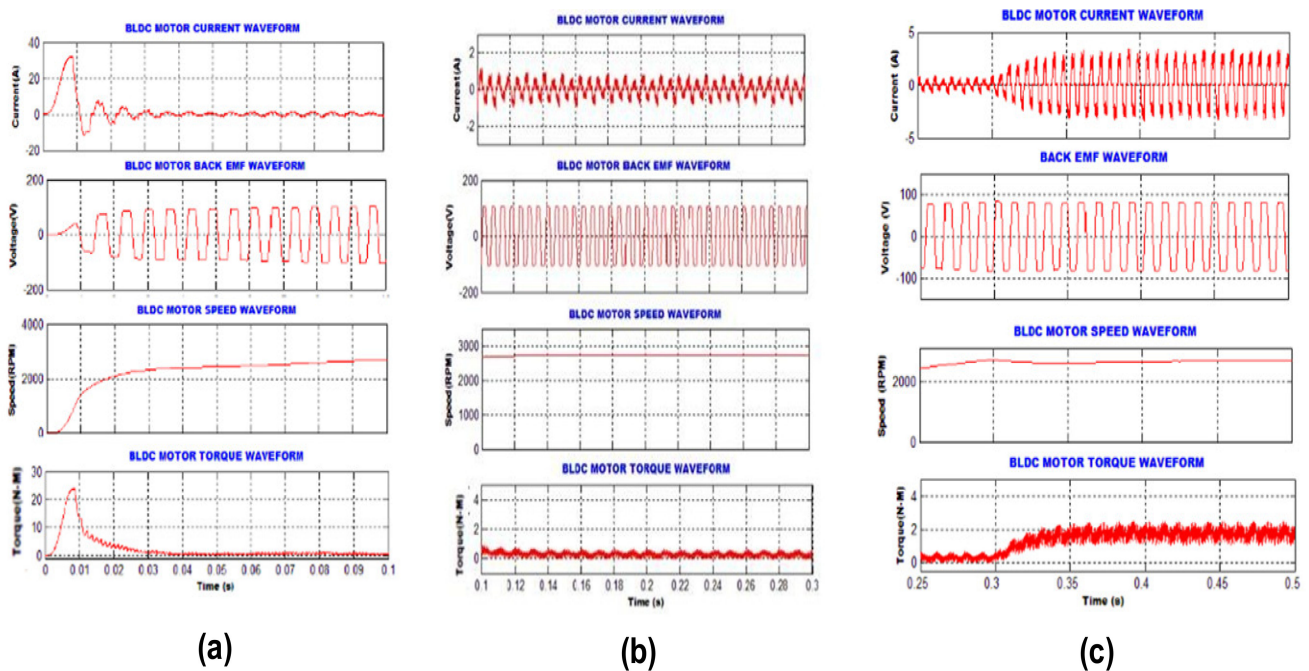


Figure 11. BLDC motor parameters with interleaved LUO converter under (a) starting, (b) running, and (c) loading conditions.

The output results shown in Figures 9–11 show that the motor current remains at zero during starting, and after $t = 0.3$ s, the motor current varies between 4 and -4 A. Likewise, the back emf (E_b) varies between 100 and -100 V during the running condition and slightly increases when the load increases in the case of the SEPIC and LUO converter. In addition, it shows a trapezoidal variation in the case of the interleaved LUO converter. The speed remains at 2800 rpm during starting and running phases. In addition, when the load is applied at $t = 0.3$ s, the torque varies about 2 Nm in the SEPIC converter and 2.5 Nm

in the LUO converter, whereas, in the interleaved LUO converter, the torque decreases to zero after $t = 0.4$ s.

4.4. Grid Output

In a grid-interactive system, it is essential to analyze the grid voltage and grid current under various operating conditions. Therefore, the grid voltage and grid current are measured during starting, running, and dynamic conditions. In this subsection, the grid voltage and grid current measured using the SEPIC converter are shown in Figure 12a–c, respectively. Likewise, the voltage and current parameters of the grid using the LUO converter are depicted in Figure 13a–c, respectively. Similarly, the obtained grid parameters such as voltage and current are depicted in Figure 14a–c, respectively.

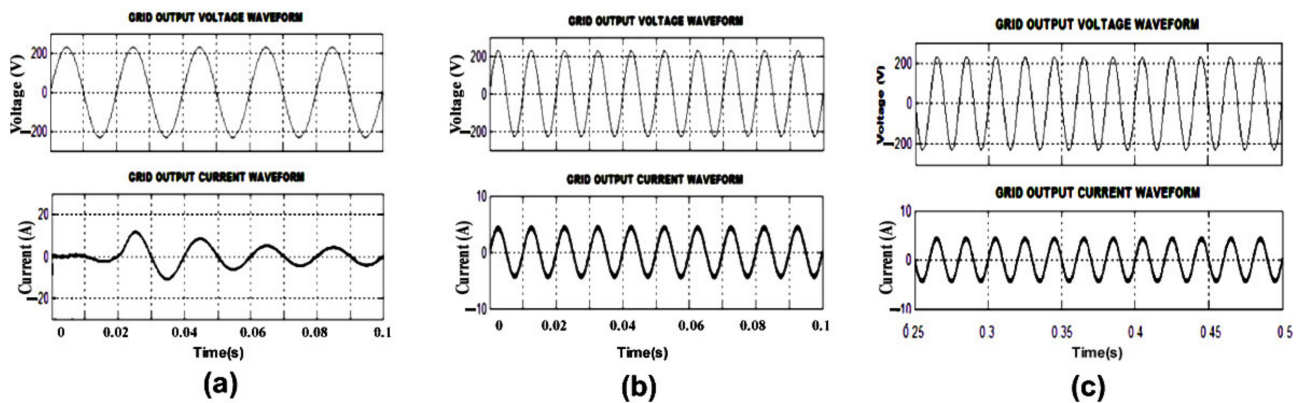


Figure 12. Grid output voltage and current using SEPIC converter under (a) starting, (b) running, and (c) loading conditions.

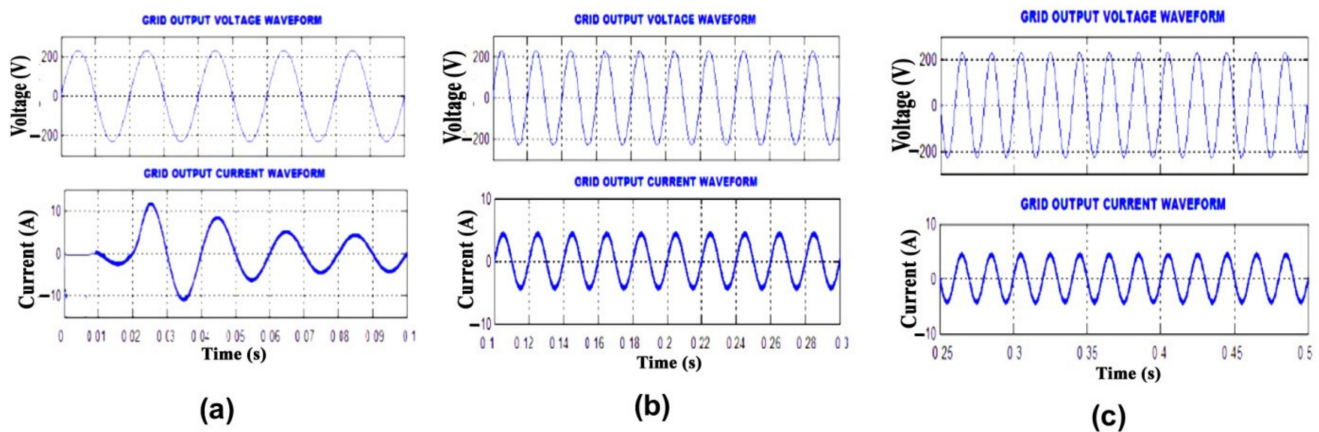


Figure 13. Grid output voltage and current using LUO converter under (a) starting, (b) running, and (c) loading conditions.

The output figures (Figures 12–14) reveal that, though the load is applied to the BLDC motor, the grid voltage and grid current remain unaffected in the case of the SEPIC, LUO, and interleaved LUO converter.

4.5. Power Quality Aspect of The Grid

The total harmonic distortion of the grid current is analyzed using the FFT analyzer. By noticing the THD values, with the implementation of the SEPIC, LUO, and interleaved LUO converters, the percentage of harmonic distortion reduces from 4.6% to 2.9%. The obtained harmonic spectra of the grid current using the SEPIC, LUO, and interleaved LUO converter are shown in Figure 15a–c, respectively.

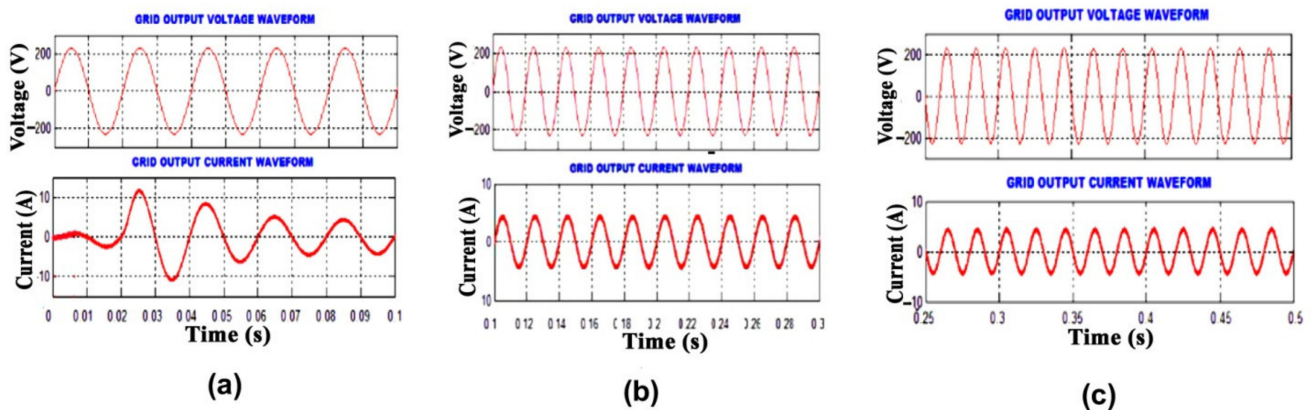


Figure 14. Grid output with interleaved LUO converter under (a) starting, (b) running, and (c) loading conditions.

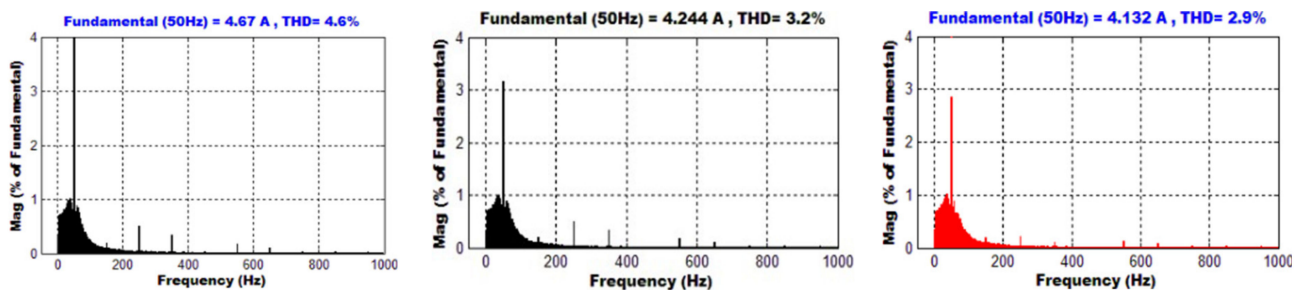


Figure 15. Harmonic spectrum of the grid current with (a) SEPIC, (b) LUO, and (c) interleaved LUO converter.

The harmonic spectrum shown in Figure 15 gives the THD values of the grid current, which is supplied to the BLDC motor. Here, the single output obtained by applying SEPIC, LUO, and interleaved LUO converters along with the whale optimization technique is presented for convenience. It is noticed that the THD reduces from 4.6% in SEPIC to 2.9% in the interleaved LUO converter. In addition, with the LUO converter, the THD is about 3.2%.

5. Conclusions

In this paper, a grid-interactive solar-fed BLDC motor for the water pumping system is developed using the MATLAB/Simulink software package. The proposed system is designed and simulated to analyze the performance of various DC/DC converters suitable for BLDC motor drive applications. The proposed method overcomes the drawbacks of the existing methods such as switching power loss, ripples, and low gain. The developed model fulfills the objectives such as the extraction of maximum power from the PV array under the condition of varying irradiance and the boosting of the output of the PV array with high gain, low ripples, and minimum power loss. The system can be operated continuously during daytime with solar power and using grid power during the night. Regarding the power quality aspect, the THD measured at the grid during the running condition of the BLDC motor is maintained under the IEEE standard limits.

Author Contributions: Data curation, P.K.B.; Formal analysis, P.W.D., P.K.B. and L.M.-P.; Investigation, J.S.O.; Methodology, J.S.O.; Software, J.S.O.; Supervision, P.W.D.; Writing—original draft, J.S.O. and P.K.B.; Writing—review & editing, P.W.D. and L.M.-P. All authors have read and agreed to the published version of the manuscript.

Funding: This research received no external funding.

Institutional Review Board Statement: Not applicable.

Informed Consent Statement: Not applicable.

Data Availability Statement: Not applicable.

Conflicts of Interest: The authors declare no conflict of interest.

References

1. Chand, V.; Kalamkar, V.R. Solar photovoltaic water pumping system—A comprehensive review. *Renew. Sustain. Energy Rev.* **2016**, *59*, 1038–1067.
2. Chandel, S.S.; Nagaraju Naik, M.; Chandel, R. Review of solar photovoltaic water pumping system technology for irrigation and community drinking water supplies. *Renew. Sustain. Energy Rev.* **2015**, *49*, 1084–1099. [[CrossRef](#)]
3. Kumar, R.; Singh, B. Grid interfaced solar PV based water pumping using brushless DC motor drive. In Proceedings of the IEEE International Conference on Power Electronics, Drives and Energy Systems, Trivandrum, India, 14–17 December 2016. [[CrossRef](#)]
4. Sridhar, R.; Vishnuram, P.; Sattianadan, D. Efficient Single Stage Photovoltaic Pumping System Using BLDC Motor with grid Power Export. *J. Sol. Energy Eng.* **2019**, *141*, 051004. [[CrossRef](#)]
5. Sharma, U.; Singh, B. Grid Interactive Bidirectional Solar PV Array Fed Water Pumping System. In Proceedings of the IEEE International Conference on Power Electronics, Drives and Energy Systems, Trivandrum, India, 14–17 December 2016. [[CrossRef](#)]
6. Murshid, S.; Singh, B. Single Stage Autonomous Solar Water Pumping System Using PMSM Drive. *IEEE Trans. Ind. Appl.* **2020**, *56*, 3985–3994. [[CrossRef](#)]
7. Shukla, S.; Singh, B. Adaptive speed estimation with fuzzy logic control for PV-grid interactive induction motor drive-based water pumping. *IET Power Electron.* **2019**, *12*, 1554–1562. [[CrossRef](#)]
8. Zhang, X.; Lu, Z. A new BLDC motor drives method based on BUCK converter for torque ripple reduction. In Proceedings of the 2006 CES/IEEE 5th International Power Electronics and Motion Control Conference, Shanghai, China, 14–16 August 2006; Volume 3, pp. 1631–1635.
9. Bist, V.; Singh, B. PFC Cuk converter-fed BLDC motor drive. *IEEE Trans. Power Electron.* **2015**, *30*, 871–887. [[CrossRef](#)]
10. Kumar, R.; Singh, B. BLDC Motor-Driven Solar PV Array-Fed Water Pumping System Employing Zeta Converter. *IEEE Trans. Ind. Appl.* **2016**, *52*, 2315–2322. [[CrossRef](#)]
11. Kumar, R.; Singh, B. Solar PV array fed cuk converter-VSI controlled BLDC motor drive for water pumping. In Proceedings of the 2014 6th IEEE Power India International Conference (PIICON), Delhi, India, 5–7 December 2014; pp. 1–31.
12. Oshaba, A.S.; Ali, E.S.; Elazim, S.M.A. MPPT Control Design of PV Generator Powered DC Motor-Pump System based on Artificial Bee Colony Algorithm. *Wseas Trans. Power Syst.* **2016**, *11*, 190–198.
13. El-samahy, A.A.; Shamseldin, M.A. Brushless DC motor tracking control using self-tuning fuzzy PID control and model reference adaptive control. *Ain Shams Eng. J.* **2018**, *9*, 341–352. [[CrossRef](#)]
14. Mishra, A.K.; Singh, B. High gain single ended inductor converter with ripple free input current for solar powered water pumping system utilizing cost-effective maximum power point tracking. *IEEE Trans. Ind. Appl.* **2019**, *55*, 6332–6343. [[CrossRef](#)]
15. Jena, P. A single stage solar PV Fed BLDC motor using ANN based MPPT for water pumping. In Proceedings of the International Conference on Computer, Electrical & Communication Engineering, Kolkata, India, 18–19 January 2019. [[CrossRef](#)]
16. Malla, S.G.; Malla, P.; Malla, J.M.R.; Singla, R.; Choudekar, P.; Koilada, R.; Sahu, M.K. Whale Optimization Algorithm for PV based Water Pumping System Driven by BLDC Motor Using Sliding Mode Controller. *IEEE J. Emerg. Sel. Top. Power Electron.* **2022**. [[CrossRef](#)]
17. Ovaiz, M.; Katta, P.; Senthil Kumar, R.; Dhiwakar, M.; Chandru, S.; Manikandan, P. Solar PV Based Super Lift LUO Converter for BLDC Motor Drive. *J. Phys. Conf. Ser.* **2021**, *1916*, 12144. [[CrossRef](#)]
18. Wu, H.-C.; Wen, M.-Y.; Wong, C.-C. Speed Control of BLDC Motors Using Hall Effect Sensors Based on DSP. In Proceedings of the International Conference on System Science and Engineering, Puli, Taiwan, 7–9 July 2016. [[CrossRef](#)]
19. Ramesh Kumar, M.; Vamsi Krishna, G.; Suresh, S. Modeling and Control of BLDC with P, PI & Fuzzy Controllers. *Int. J. Adv. Res. Electr. Electron. Instrum. Eng.* **2017**, *6*, 414–422.
20. Killi, M.; Samanta, S. Modified perturb and observe MPPT algorithm for drift avoidance in photovoltaic systems. *IEEE Trans. Ind. Electron.* **2015**, *62*, 5549–5559. [[CrossRef](#)]
21. Terki, A.; Moussi, A.; Betka, A.; Terki, N. An improved efficiency of fuzzy logic control of PMBLDC for PV pumping system. *Appl. Math. Model.* **2012**, *36*, 934–944. [[CrossRef](#)]
22. Mohanty, S.; Subudhi, B.; Ray, P.K. A New MPPT Design Using Grey Wolf Optimization Technique for Photovoltaic System under Partial Shading Conditions. *IEEE Trans. Sustain. Energy* **2015**, *7*, 181–188. [[CrossRef](#)]
23. Darcy Gnana Jegha, A.; Subathra, M.S.P.; Kumar, N.M. Optimally tuned Interleaved Luo Converter based for PV array fed BLDC driven Centrifugal using Whale Optimization Algorithm -A Resilient solution for powering Agricultural Loads. *Electronics* **2020**, *9*, 1445. [[CrossRef](#)]